

1 **Nano-engineering chitosan particles to sustain the release of promethazine from orodispersables**

2 Authors:- Arwa Matoug Elwerfalli^a, Ali Al-Kinani^a, Raid Alany^a, Amr ElShaer^{a,‡}

3 ^aDrug Discovery, Delivery and Patient Care (DDDPC), School of Pharmacy and Chemistry, Kingston University
4 London, Kingston Upon Thames, Surrey, KT1 2EE, UK

5

6 **‡ Corresponding author**

7

8 **Dr Amr ElShaer**

9 **Drug Discovery, Delivery and Patient Care (DDDPC)**

10 **School of Pharmacy and Chemistry**

11 **Kingston University London**

12 **Penrhyn Road, Kingston Upon Thames,**

13 **Surrey, KT1 2EE, UK**

14 **Email: a.elsaer@kingston.ac.uk**

15 **T +44 (0)20 8417 7416 (Internal: 67416)**

16

17

18

19

20

21

22

23

24

25

26

27

28

29

30

31

32 **Abstract**

33 Orally dispersing tablets (ODTs), also known as orodispersibles, were first introduced into the market in
34 1980s to overcome dysphagia problems amongst paediatrics and geriatrics. Despite their abilities to avoid
35 swallowing difficulties, frequency of dosing stood as a barrier for these formulations. The aim of the current
36 study is to produce and optimize a sustained release orally disintegrating tablets (SR-ODT), with the aid of
37 chitosan. A design of experiment (DoE) was first performed using Minitab to determine the effect of five
38 independent variables on three dependent responses when producing the nanoparticles using ionotopic
39 gelation. The variables studied were (tripolyphosphate concentration TPP, Chitosan concentration CS, acetic
40 acid concentration, Chitosan: tripolyphosphate ratios and stirring time) and the responses were (particle
41 size, surface charge and encapsulation efficiency). A formulation with optimum particle size, surface charge
42 and encapsulation efficiency was prepared and further coated with polyvinylpyrrolidone (PVP), polyethylene
43 glycol (PEG) and polyethylene co-acrylic acid (PEAA). Minitab studies revealed that the nanoparticles' particle
44 size was affected by most of the independent variables except stirring time and the ratios of CS to TPP. The
45 optimized nanoparticles showed particle size of 153.8 ± 14 nm, surface charge of 31.4 ± 0.9 mV and
46 encapsulation efficiency of $99.7 \pm 0.06\%$. The DSC showed that PMZ was solubilized within chitosan
47 nanoparticle, whereas SEM images indicated that all the samples were spherical in shape with smooth
48 surface and had similar size to that measured by DLS. After coating and dispersing into the tablets' matrices,
49 the tablets were evaluated to determine the friability, disintegration time and tensile strength. All tablets
50 were at an appropriate friability (less than 1%) and had tensile strength above 2.5 N/mm^2 . Besides, all the
51 tablets managed to disintegrate within 40 seconds while sustaining the drug release over 24 hours.

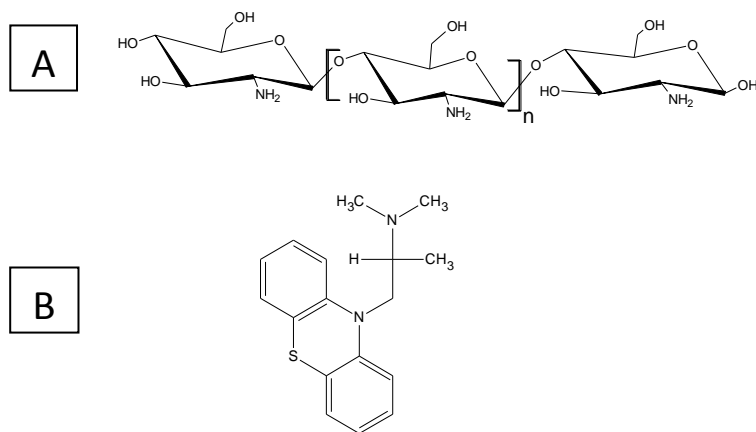
52 **Keywords:-** orally disintegrating tablets, chitosan, design of experiment, sustained release, polymers.

53 **1. Introduction**

54
55 Oral drug delivery is the most common route of drug administration and the last 10 years have witnessed
56 significant developments in oral formulations as novel dosage forms and manufacture technologies have
57 been introduced. A new dosage form known as orally dispersing tablets (ODTs) was introduced in 1980s to
58 overcome a common clinical problem known as dysphagia among paediatric and geriatric populations. The
59 clinical study conducted by Lindgren and Janzon (1991) showed that 35% of patients aged between 50 and
60 69 suffered from some degree of dysphagia. It has also been established that nearly 1 in 5 patients avoid
61 taking oral medication due to swallowing difficulties (Lindgren & Janzon, 1991; Krause & Breitreutz, 2008).
62 Dysphagia is also associated with poor patient compliance, the latter is a foremost medical issue that costs
63 more than \$290 billion a year (Fulzele, Moe & Hamed, 2012.; Gryczke, Schminke, Maniruzzaman, Beck, &
64 Douroumis, 2011). Therefore, the need for a viable oral disintegrating formulation is paramount. ODTs are
65 also termed as orodispersible in the European Pharmacopoeia and defined as 'tablets that disperse or
66 disintegrate in less than 3 mins in oral cavity before it is turned into a paste that can be easily swallowed
67 (Hirani, Rathod, & Vadalía, 2009; Beckert, Lehmann, and Schmidt, 1996; Wagh, Kothawade, Salunkhe,
68 Chavan, & Daga. 2011)

69 The first generation of ODTs achieved a lot of success, with various properties and characteristics of ODTs
70 offered by the numerous preparation techniques. Nonetheless, the first generation of ODTs failed to
71 overcome challenges such as delivering acid labile drugs, macromolecule and high doses. A lot of studies
72 investigated new approaches to circumvent these technical issues. Further research into ODTs resulted in
73 the production of sustained-release oral disintegrating tablet (SR-ODT) with the aim of improving the oral
74 disintegrating drug delivery system. This is where the tablet disintegrates completely in the mouth but also

75 sustain the duration of action. This will reduce the frequency of dosing and will enhance patient adherence
 76 to ultimately improve the quality of lifestyle for patients (Abdul & Poddar. 2004). Many approaches such as
 77 microencapsulation (Sunitha, & Amareshwar. 2010; Shazly, Tawfeek, Ibrahim, Auda, & El-Mahdy, 2013),
 78 nanoparticles (Kondo, Ito, Niwa, & Danjo, 2013) ion exchange resins (Chen et al., 1992; Gokhale and
 79 Sundararajan., 2013) and stimuli-responsive polymers (Beckert, Lehmann, and Schmidt 1996; Abbaspour,
 80 Sadeghi & Garekani, 2008) have been adapted to control the drug release across ODTs.
 81 Recently, chitosan (CS) has attracted great attention in pharmaceutical industry to produce sustained release
 82 delivery systems, due to its biodegradability and biocompatibility, in addition to, its nontoxicity (Jiang, Pan,
 83 Cao, Jiang, Hua, & Zhu, 2012). Chitosan is considered as one of the most abundant natural polysaccharide
 84 (Jiang, Pan, Cao, Hua, & Zhu, X.2012; Bugnicourt, Alcouffe, & Ladavière. 2014) which is chemically known as a
 85 β -(1,4)-2-acetamido-D-glucose and β -(1,4)-2-amino- D-glucose and comprises of of glucosamine
 86 copolymerised with N-acetyl glucosamine (Kaloti, & Bohidar 2010), the primary amino group and two free
 87 hydroxyl groups on carbon (C8) provides a positive charge on the surface (Fig 1A) .CS has a pka of 6.3-7 and is
 88 only soluble in aqueous media at low pH, which might lead to a premature release of the drug.



89

90 Fig 1:- Chemical structure of chitosan (A) and promethazine (B).

91

92 Chitosan is considered to be safe, as low molecular weight chitosans are eliminated easily by the kidney,
 93 while, the larger molecular weight polymers are degraded by chemical and enzymatic catalysis, furthermore
 94 the enzyme catalysis is dependent on the availability of chitosan amino group. The ability of CS to form nano-
 95 microparticulate systems depends on its ability to form covalent cross-linking between the chitosan chain
 96 and the functional cross-linking agent such as polyethylene glycol (PEG), dicarboxylic acid or
 97 tripolyphosphate. Patel et al (2013) utilised CS to develop a sustained delivery system of Rifampicin.
 98 Rifampicin nanoparticles were prepared by ionic gelation method in presence of tween-80 and
 99 tripolyphosphate to act as surfactant and cross-linker respectively. The prepared nanoparticulate system
 100 had particle sizes of 181nm – 383nm and managed to sustain rifampicin release for 28-34 hours. It was
 101 further concluded that extensively cross-linked nanoparticles displayed decreased drug release rates (Patel,
 102 Parikh, & Aboti, 2013). Li-Q et al attempted a new microencapsulation technique to produce a SR ODT for
 103 scopolamine hydrobromide, where the nanoparticles are encapsulated to produce a sustained-release
 104 effect. The particles were produced using ionotropic gelation followed by spray drying, *in vitro* studies
 105 showed that tablets have disintegration time of <45s, particle size of 300 nm and managed to release 90%
 106 of the drug within 90min (Li, , et al., 2011). Other studies demonstrated that CS alone might not be able to

107 sustain the drug release. Abdelbary et al conducted *in vitro* and *in vivo* evaluation of microencapsulated
108 glipizide for orally extended delivery. After preparing glipizide microcapsules by ionotropic gelation
109 technique, the microcapsules were coated with alginate alone or combined with carbomer 934P. It was
110 concluded that the extended release of drug depended on the composition of the outer coat. Microparticles
111 coated with sodium alginate alone or in combination with low molecular weight (LMW) chitosan were found
112 to be unsuccessful at retarding the drug release. However, when LMW chitosan was replaced by high
113 molecular weight chitosan, approximately 80% of the drug was released after 8 hours. Other polymers were
114 employed in preparing sustained release particulate systems across ODTs. The production of ketoprofen
115 controlled release ODT was investigated using Eudragit RS-30D. The pellets were directly compressed and
116 the *in vitro* studies revealed disintegration time of 30s. (Wei, Yang, & Luan, 2013).

117 Promethazine (PMZ) is the model drug used in this study (Figure 1B); pharmacologically PMZ is used as a H1
118 and alpha-adrenergic receptor antagonist, with a limited effect on dopaminergic receptor. PMZ is used
119 widely to treat allergy symptoms such as itching, runny nose, sneezing, itchy or watery eyes, hives, and itchy
120 skin rashes (Kavanagh, Grant et al. 2012). PMZ also prevents motion sickness and treats nausea, vomiting
121 and pain after surgery. Furthermore, PMZ is used as a sedative or sleep aid (Ford, Rubinstein et al. 1985).
122 Pfeil and colleagues have found that PMZ is considered as the mostly prescribed antiemetic in the US, as
123 more than 90% of the prescriptions for antiemetic's are promethazine in comparison to other antiemetic on
124 the market (Adolph, et al., 2012)

125 Due to the wide interest and promising results obtained when using chitosan to produce a sustained-release
126 nanoparticles the aim of this study is to produce a sustained release nanoparticle system, to be integrated
127 into an oral disintegrating tablet matrix. The study also aims to compare the effect of different coating
128 polymers on the drug release profiles of PMZ and their toxicity on Caco-2 cells.

129 **2. Material and method**

130 **2.1. Material**

131 Promethazine hydrochloride (MW 320.88) was purchased from Tokyo chemical industry co, (Tokoyo,Japan).
132 Chitosan (CS) of medium molecular weight (MW, 190,000-310,000 Da) and with degree of deacetylation
133 (DD) of 75%, Sodium tripolyphosphate (TPP), Polyethylene glycol PEG (Mn 80,000 units),
134 Polyvinylpyrrolidone (PVP), Poly ethylene co acrylic acid, Magnesium stearate fluka (analytical standard
135 $\geq 99.5\%$) and D (+)-Lactose Monohydrate were all purchased from Sigma-Aldrich (Mo, USA), L-substituted
136 hydroxypropylcellulose; LH-B1 -MW, 140,000 Da, 11% hydroxypropoxy content, degree of polymerization of
137 790 and 0.2 molar substitution- was a gift from Shin-Etsu Chemical co.td. (Tokyo, Japan).

138 The Caco-2 cell lines were obtained from Sigma Aldrich (Dorset, UK), while Essential Eagle's Medium (EMEM)
139 L-glutamine, fetal bovine serum Penicillin Streptomycin were all purchased from Fisher Scientific
140 (Loughborough, UK).

141 **2.2 Methods**

142 **2.2.1. Design of experiment (DoE)**

143

144 A factorial design of experiment was used to determine the effect of six dependent variables on three
145 responses and to optimize the experiment conditions to achieve a nanoparticulate system with small particle
146 size (100-300nm) with maximum drug loading. A fractional factorial design was generated where the

147 variables used in this design were CS concentration (0.1-0.5% w/v), TPP concentration (0.1-.05% w/v), acetic
 148 acid concentration(0.5-1% v/v), CS:TPP (5:1- 5:2) ratio and drug concentration(0.4-0.8 mg/mL) and stirring
 149 time (30- 90 mins) while the responses were particle size, surface charge and drug loading. A total of 16
 150 experiments were performed in order to optimise the properties of nanoparticles produced (Table 1). In
 151 order to minimise the effect of extraneous factors on actual responses, the experimental runs were
 152 randomized. The response surface model was evaluated using equation (1) where Y is the response value
 153 predicted by the model of which α_0 is a constant whereas α_i , α_{ij} , α_{ijh} are linear, 2-way and 3-way interaction
 154 coefficient respectively. A response optimizer was used to obtain optimum conditions to produce
 155 nanoparticles in the size range of (100-250nm) and maximum drug load. The experimental design and data
 156 analysis were carried out using Minitab statistical package (Minitab® 17.1.0, Minitab inc., PA, USA)

157 $Y = \alpha_0 + \sum \alpha_i X_i + \sum \alpha_{ij} X_{ij} + \sum \alpha_{ijh} X_{ijh}$ Equation 1

158 Table 1:- Matrix of 16 runs used to optimise chitosan nanoparticles

Number of runs	CS-conc (%w/v)	TPP-conc (%w/v)	CS:TPP ratio	Stirring time (min)	drug concentration (mg/ml)	acetic acid (%v/v)
1	0.5	0.1	5:2	30	0.4	0.5
2	0.1	0.1	5:1	30	0.4	1.0
3	0.1	0.5	5:2	30	0.4	1.0
4	0.1	0.1	5:2	30	0.8	0.5
5	0.1	0.5	5:2	90	0.4	0.5
6	0.1	0.1	5:1	90	0.4	0.5
7	0.1	0.5	5:1	90	0.8	1.0
8	0.1	0.1	5:2	90	0.8	1.0
9	0.5	0.5	5:1	30	0.4	0.5
10	0.5	0.1	5:1	30	0.8	1.0
11	0.1	0.5	5:1	90	0.8	0.5
12	0.5	0.1	5:1	90	0.8	0.5
13	0.5	0.5	5:2	90	0.8	0.5
14	0.5	0.5	5:2	30	0.8	0.1
15	0.5	0.5	5:1	90	0.4	0.1
16	0.5	0.1	5:2	90	0.8	0.1

159

160 **2.2.2. Preparation of CS/TPP nanoparticles**

161 CS/TPP nanoparticles, were prepared using ionotropic gelation method (Calvo, Remunan, Vila, & Alonso,
 162 ,1997) CS solution was prepared in concentrations of (0.1%-0.5%w/v) in acetic acid solution (0.5%-1% v/v). A
 163 Second solution of TPP was prepared at concentration of (0.1%-0.5%w/v) in deionized water. After filtration
 164 using 0.24µm syringe filters (Millex®-HA,Merck KGaA, Germany), TPP was added to CS solution dropwise
 165 until ratios of (5:1 and 5:2) were achieved. The obtained CS:TPP solutions were stirred under ambient
 166 conditions for (30-90 mins), which led to spontaneous formation of nanoparticles. The nanoparticles were
 167 obtained by centrifugation of the sample at 20.000 rpm for 30min at temperature of 4°C using (SIGMA 3-
 168 30K, SciQuip, Germany) and the pellets obtained were washed by dispersing the pellets in distilled water and
 169 centrifugation for 15min. (Calvo, Remunan, Vila, & Alonso, ,1997; Najafabadi, Abdouss, & Faghihi, 2014;
 170 Makhija, & Vavia 2002)

171 PMZ nanoparticles were prepared using similar method. Where the drug (PMZ) was added in concentration
172 of (0.4-0.8mg/mL) to the CS solution under magnetic stirring for 30min (Calvo, Remunan, Vila, & Alonso,
173 ,1997; Najafabadi, Abdouss, & Faghihi, 2014; Makhija, & Vavia 2002) before adding TPP solution.

174 **2.2.3. Preparation of CS and PMZ coated nanoparticles**

175 After optimizing CS nanoparticles, the obtained particles were further coated using three polymers namely;
176 PEG, PVP and PEAA to sustain the drug release across the nanoparticulate system. CS/TPP coated
177 nanoparticles were prepared by adding the polymer in concentration of (10-20mg/ml) to the CS/PMZ
178 solution prior to initiating the ionic gelation by adding TPP.

179

180 **2.2.4. Tablet formulation**

181 The prepared nanoparticles were embedded inside orally disintegrating tablet matrix made of 25% LH-B1,
182 1% lubricant (Magnesium stearate), nanoparticles contacting 5% drug (10mg or equivalent of PMZ) and 69%
183 diluent (D (+)-Lactose Monohydrate), all ingredients were mixed using (WAB Turbula®, willy A, Bachofen AG,
184 Switzerland) and compressed using uniaxial hydraulic press (Specac tablet presser, Slough, UK) and split die
185 which prevents mechanical failure by allowing triaxial decompression. The prepared tablets were cylindrical
186 with a diameter of 13 mm and weight of around 500 mg. Tablets were left in desiccators until
187 characterisation studies were performed.

188 **2.2.5. HPLC Analysis**

189 PMZ analysis was performed using (Shimadzu, Shimadzu Corporation, Japan) HPLC system. RP-C18 column
190 (250x4.6 mm, 5µm) was used to retain PMZ using mobile phase made of acetonitrile and 0.354%v/v
191 triethylamine solution (pH of 2.5 adjusted with orthophosphoric acid), in a ratio of 41:59 (v/v) respectively.
192 Mobile phase was pumped using a quaternary pump at a flow rate of 1ml/min. PMZ had retention time of
193 2.36 ± 0.01 mins when analysed at λ_{max} of 250 nm. The analytical method was validated according to
194 International Conference of Harmonization (ICH) guidelines. Calibration curve was established at
195 concentrations ranges of 10-200µm with coefficient of variation ($R^2=0.99$) and curve equation ($y = 56839x +$
196 10^6).

197 **2.2.6. Nanoparticles characterisation**

198 **2.2.6.1. Dynamic light scattering transmission:**

199 Particle size distribution, polydispersion and zeta potential (ξ) of the nanoparticles were analysed through
200 DLS, the analyses were performed using diluted suspension of nanoparticles at 1:10 v/v dilution using
201 Malvern Zetasizer 300HSA (Malvern Instruments, UK) fitted with a detector at angle of 90°. All the analysis
202 were carried out at room temperature and expressed as mean \pm SD of three readings. Zeta potential (ξ) was
203 measured in triplicates by photon correlation spectroscopy (PCS) using Malvern Zetasizer 300HS_A (Malvern
204 Instruments, UK).

205 **2.2.6.2. Thermogravimetric analysis (TGA)**

206 A thermogravimetric analyser (Toledo SDTA/TGA 851e, UK) was used in this study to measure the moisture
207 content and decomposition temperature of PMZ and its prepared nanoparticles. 5- 10 mg of samples were
208 loaded on to an open pan and were analysed between 20-500 °C at 10 °C/min scanning rate and under
209 nitrogen stream. Software (STAR[®]SW 10.00) was used to analyse the obtained thermograms.

210 **2.2.6.3. Differential scanning calorimetry (DSC).**

211 Differential scanning calorimeter (Mettler Toledo, DSC822^e, UK) was used to explore the physical
212 transformation of PMZ and the prepared nanoparticles by determining the heat flow from and to the
213 sample. Approximately 2-5 mg of the samples were weighted and transferred to an aluminum sample pan
214 (50 μ L capacity). Intra cooler 2P system was used to initially cool the samples to 25 $^{\circ}$ C and then sample
215 heated to 250 $^{\circ}$ C at a rate of 10 $^{\circ}$ C/min. Nitrogen was used as a purge gas at a flow rate of 20 mL/min. The
216 obtained thermograms were analysed using STAR^eSW 10.00 software. All experiments were performed in
217 triplicate and an empty aluminum pan was used as a reference cell for all the measurements. Both sample
218 and reference pans were covered by aluminum lids and pierced on the top.

219

220 **2.2.6.4. Scanning electron microscopy (SEM)**

221 Scanning electron microscopy (SEM, Zeiss Evo50- Oxford instrument, UK) was used to study the surface
222 morphology of PMZ and the prepared nanoparticles. Samples were prepared by sprinkling PMZ or adding a
223 drop of nanoparticles suspension onto specimen stubs. After drying the suspension, stubs were loaded onto
224 a universal specimen holder. In order to enable electricity conduction, samples were coated with a fine layer
225 of gold using a sputter coater (Polaron SC500, Polaron Equipment, Watford, UK) at 20 mA for three mins at
226 low vacuum and in the presence of argon gas (Polaron Equipment, Watford, UK).

227 **2.2.6.5. Determination of encapsulation efficiency of nanoparticles using HPLC.**

228 HPLC method (section 2.2.5) was used to determine the percentage of encapsulation efficiency in the
229 prepared nanoparticles. In this process, the supernatant of the nanoparticle that was collected during
230 centrifugation was filtered and analysed using HPLC and equation (2) was used to calculate % PMZ
231 encapsulation efficiency.

232
$$\%Drug\ encapsulation\ efficiency = \frac{total\ amount\ of\ drug - free\ amount\ of\ drug}{total\ amount\ of\ drug} \times 100 \text{ Equation 2}$$

233 **2.2.6.6. Sulforhodamine B (SRB) cytotoxic assay.**

234 **2.2.6.6.1 Caco-2 cells culture**

235 The Caco-2 cell line was grown in Minimum Essential Eagle's Medium (EMEM) that was supplemented with
236 200 mM L-glutamine, 10% fetal bovine serum, 10,000 U of Penicillin and 10 mg/mL of Streptomycin. Caco-2
237 cells were maintained in humidified atmosphere of 5% \pm 0.5 CO₂ and at a temperature of 37 \pm 0.5 $^{\circ}$ C. All
238 experiments were performed between passages 57-60.

239 **2.2.6.6.2 Sulforhodamine B (SRB) cytotoxic assay**

240 Cytotoxic effect of the prepared nanoparticles was evaluated using Sulforhodamine B (SRB). SRB protocol
241 was adapted from Vichai and Kirtikara (2006). Briefly, Caco-2 cells were seeded in a 96 well plate at a density
242 of 20,000 cell/well. The cells were incubated for 24 hours at a temperature of 37 \pm 0.5 $^{\circ}$ C and humidified
243 atmosphere of 5% \pm 0.5 CO₂. The nanoparticles were centrifuged, and the supernatant discarded, the
244 nanoparticles were re-suspended in the treatment media prior the test. The cytotoxic assay was evaluated
245 for the following concentration of 40 mg/mL, 20 mg/mL and 10 mg/mL of nanoparticles suspension. After
246 the 24 hours cultured period, the cell media was removed and 100 μ L of the test materials were added. The
247 test materials used were: nanoparticles (different concentration) suspension, the negative control

248 (treatment media only) and positive control (50µm trytona X). This followed by another 24 hours incubation
249 time using the same condition above. After the second incubation, the cells were fixed by treatment with
250 100 µL of 10% Trichloroacetic acid (TCA) for 1 hour. Then, the TCA was washed out thoroughly with water
251 and left to dry overnight. SRB dye was added to each well (100 µL of 0.4% SRB) for 30 mins then washed out
252 using 1% acetic acid and the plate was kept for drying overnight. The SRB dye was de-stained using 100 µL
253 tris buffer and the optical density was measured at 565 nm using Epoch Spectrophotometer (Bio TeK, VT,
254 USA).

255

256 **2.2.7. Tablet evaluation**

257 **2.2.7.1. Measurement of tablet tensile strength**

258 The force required to crush the prepared tablets was measured using tablet hardness apparatus (Schleuniger
259 4M, Thun, Switzerland). The measured force was used to determine the tablet tensile strength using
260 equation (2) (Digital Vernier Dial Caliper Gauge Micro Meter 150mm(UK).

$$261 \quad \sigma = \frac{2F_c}{\pi dt} \text{ Equation 3}$$

262 Where σ is the tablet tensile strength, F_c is the crushing force required to break the tablet, d is the tablet
263 diameter and t is the tablet thickness. All measurements were done in triplicate.

264 **2.2.7.2. Measurement of tablet disintegration time**

265 Disintegration time is the time required for tablets to disintegrate completely without leaving any solid
266 residue. *In vitro* disintegration time was evaluated using US pharmacopoeia monograph (<701>
267 disintegration). Erweka ZT3, Appartebau, GMBH ,Husenstamm, Germany) was used in this study as a
268 disintegration apparatus and distilled water (800 ml) as disintegration medium; the disintegration medium
269 temperature was maintained at 37 ± 0.5 °C by thermostat. Six tablets were placed in the basket rack
270 assembly and covered by transparent plastic disks. The disintegration time was taken as the time required
271 for tablets to disintegrate completely without leaving any solid residue. All the measurements were carried
272 out six times and presented as mean \pm standard deviation.

273

274 **2.2.7.3. Measurement of friability**

275 The friability will be determined as a percentage of weight loss in a random sample of tablets. A random
276 sample of tablets will be weighed on an analytical balance to achieve a total mass weight of (>5g), based on
277 the British pharmacopoeia guidelines for friability testing. Then tablets were placed in a friabilator (Erweka
278 AR 400 ,Germany) for 4 min at 25rpm, after that the tablets were dusted and reweighed. Percentage
279 friability will be calculated using equation (3)

$$280 \quad \% \text{ friability} = \frac{\text{initial weight} - \text{final weight}}{\text{initial weight}} * 100 \text{ Equation 4}$$

281 **2.2.7.4. Dissolution test (Drug release)**

282 The dissolution of ODTs tablets containing 10 mg of PMZ or equivalent amount of PMZ nanoparticles was
283 evaluated using USP II paddle method (Caleva 9ST, Germany). The prepared tablets were placed into
284 dissolution vessels containing 900 mL of 0.01M HCL buffer (pH 1.2) and the dissolution media was
285 maintained at $37^\circ\text{C} \pm 0.5^\circ\text{C}$ and stirred at 50 rpm. 5mL of samples were collected at a predetermined time
286 intervals (5min,10min, 15min, 20min, 30min, 60min, 90min, 120min, 6hr, 22hr, 24hr) then filtered through

287 0.45 µm Millipore filters. The dissolution media was replaced by 5mL of fresh dissolution media in order to
288 maintain a constant volume. After proper dilution samples were analysed by HPLC method (section 2.2.5).

289 **2.2.7.5. Statistical analysis**

290 Formulation were prepared and analysed in triplicate and the results were expressed as ± mean standard
291 deviation. Graph pad Prism® 6 (version 6.5) was used to analyse the date obtained, the results were
292 analysed by two-way ANOVA (Tukey) $p < 0.05$ was considered to be statistically significant for this analysis.
293

294 **3. Results and discussion**

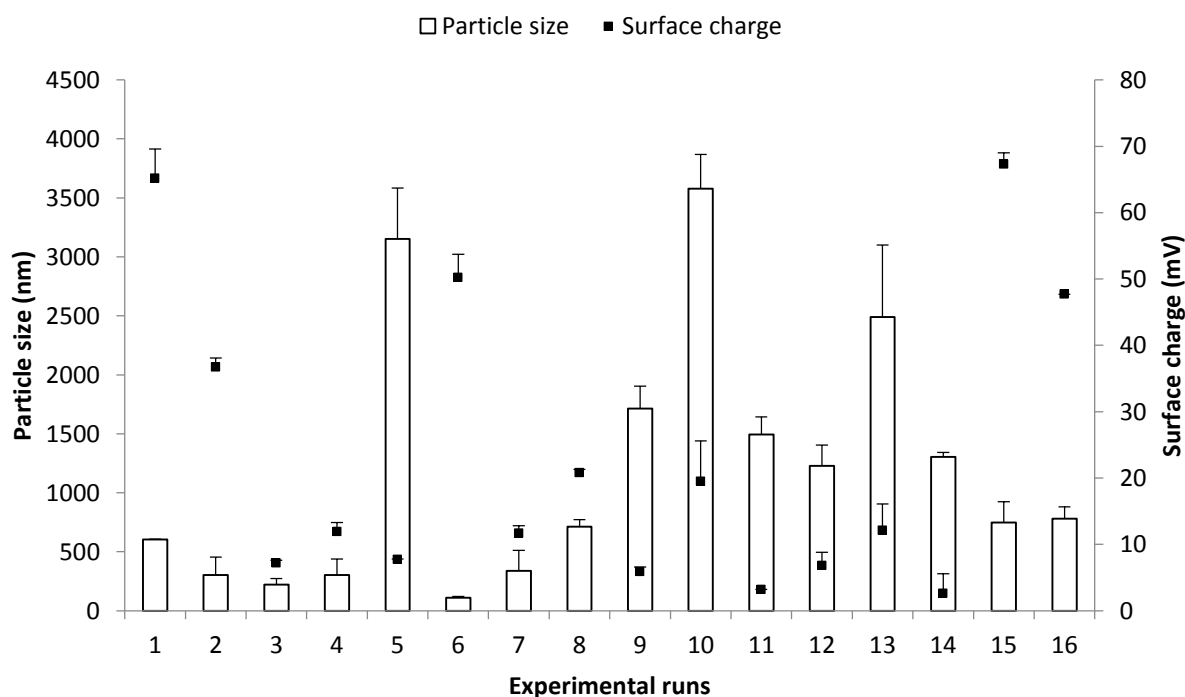
295

296 **3.1. Design of experiment (DoE)**

297

298 Two-level factorial design of experiment was performed, with the use of six parameters (CS concentration,
299 TPP concentration, acetic acid concentration, stirring time and CS:TPP ratio), where Minitab generated 16
300 experiments, that were produced and evaluated based on the three variables; particle size, surface charge (ξ)
301 (Fig 2) and encapsulation efficiency (EE). The DoE approach was employed in order to optimize the
302 experiment conditions and produce a sample with the desired properties, a small particle size (100-300nm)
303 and high encapsulation efficiency. High encapsulation efficiency means use of fewer amounts of
304 nanoparticles, hence tablet characteristics would not be compromised especially disintegration time. In
305 other words, poor entrapment efficiency would require high amounts of the polymeric nanoparticles which
306 would bind strongly to other excipients in the tablet matrix and tablet disintegration would fail. After
307 evaluation of all samples, the data was uploaded into Minitab, to statistically analyses the data obtained,
308 Minitab generated a number of graphs to show the impact of each variable on the responses.

309



310

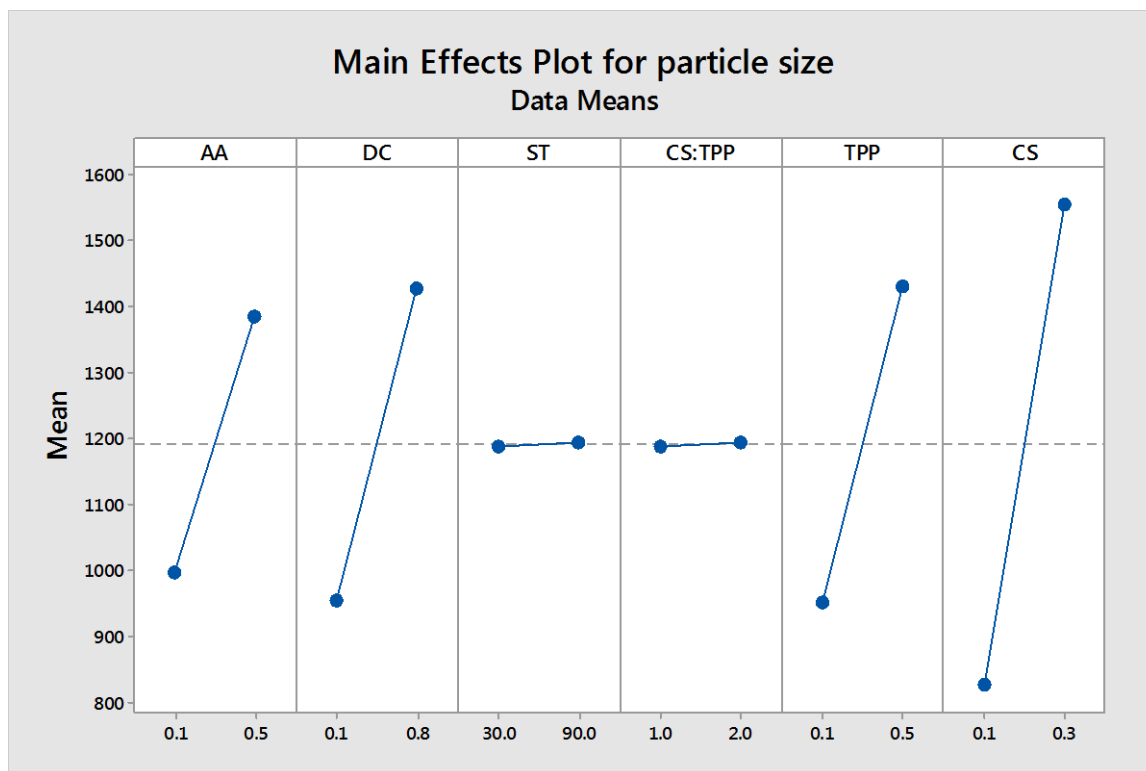
311 *Fig 2:- Summary of the effect of various variables on the particle size and surface charge*

312 **3.1.1. The effect of different parameters on particle size**

313

314 Particle size is an important determinant of drug bioavailability as it is believed that nanoparticles with size
315 less than 100 nm has 3-fold arterial uptake compared to larger particles (Song, Labhasetwar, Cui,
316 Underwood, & Levy, 1998). From formulation aspect, particles with smaller size will have a larger surface
317 area and increasing the surface area will enhance the ability of the particles to withstand the compression

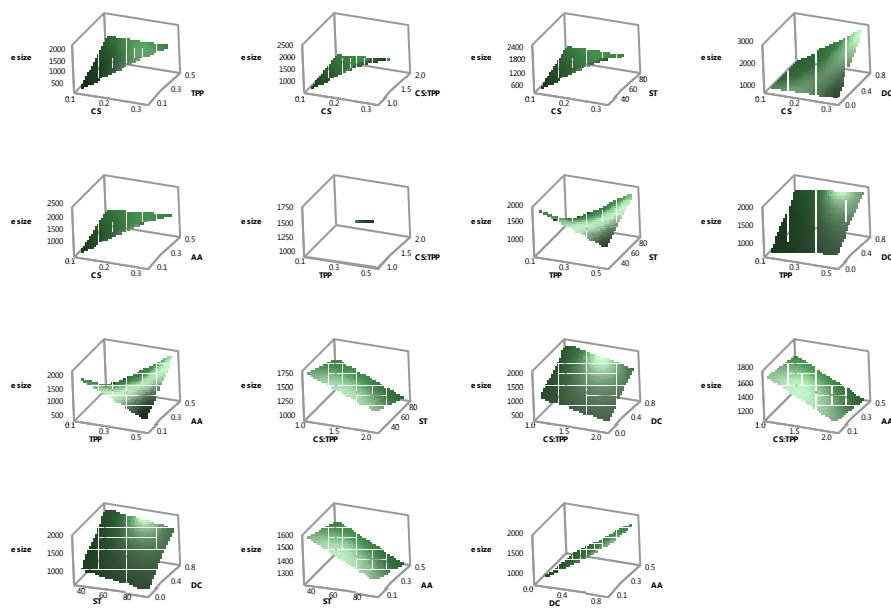
318 force during the tableting process by decreasing the overall compression pressure per particle, hence
 319 optimising the particle size is a mandate in the current study. Formation of CS nanoparticles depends on the
 320 ability of the polymer to form intermolecular cross-linkages with polyanions such as TPP. The extent of
 321 Intermolecular cross-linkages between the phosphate groups of TPP and the amino groups of CS will control
 322 and modulate the properties of CS nanoparticles prepared. The current study looked at the effect of six
 323 independent variables on the size of CS particulate system. The DoE study demonstrated that particle size is
 324 dramatically influenced by most of the variables; CS concentration, acetic acid concentrations, drug
 325 concentrations and TPP concentrations. On the other hand, stirring time and CS:TPP ration did not show any
 326 impact on the size of CS nanoparticles (Figs 3 &4).



327

328 Fig 3:- Main effects plot showing the influence of the independent variables on CS particle size

Surface Plots of particle size



329

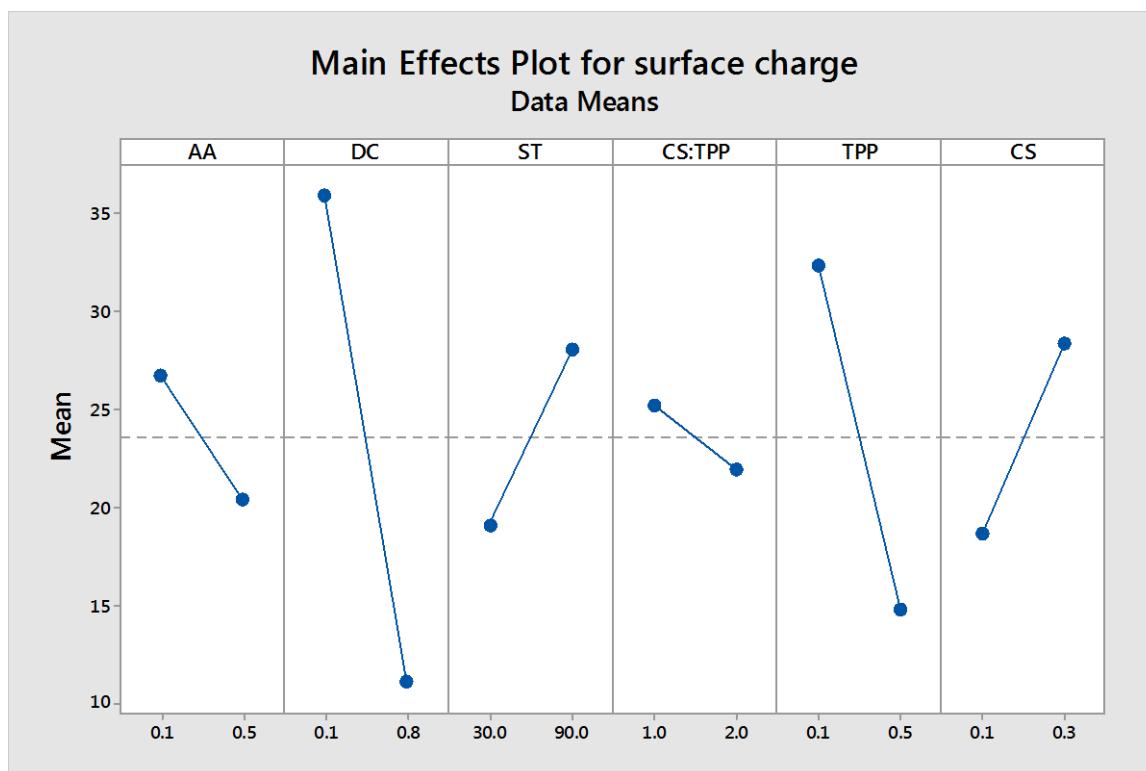
330 *Fig 4:-Response surface plots of interaction effects between different variables and their effect on CS particle*
 331 *size. Hold values are 0.20 for CS, 0.30 for TPP, 1.50 for CS:TPP, 60.00 for ST, 0.45 for DC and 0.30 for AA.*

332 According to the main effect plot (Fig 3), CS concentrations had the foremost influence on the particles size
 333 of the prepared nanoparticles. Increasing CS concentration was associated with an increase in the average
 334 particle size of the nanoparticles. Possibly increasing the concentration of CS results in a viscosity
 335 increase, which in turn will affect the shear capacity of homogenization leading to the formation of
 336 aggregates with larger particle size (Hong et al., 2014; Bugnicourt, Alcouffe, & Ladavière. 2014). Similar
 337 findings were also reported by Bugnicourt et al., 2014 (Bugnicourt, Alcouffe, & Ladavière. 2014). Looking at
 338 the effect of TPP concentration on particle size, it was demonstrated that the higher the concentration of
 339 TPP, the larger the particle size, this is because of the stiffening of the cross-linking bonds between TPP and
 340 CS associated with the rise of the triphosphoric ions (Patel, Parikh, & Aboti, 2013). The increase in the
 341 drug concentration led to a decrease in the particle size, this could be attributed to the competition between
 342 PMZ and CS cations to bind with TPP phosphoric ions which in turn will decrease the intermolecular cross
 343 linkage between CS and TPP and hence the formation of larger particles. Similar pattern was observed when
 344 higher concentration of acetic acid was used to solubilise CS; increasing the drug concentration will increase
 345 the negative charge in the sample, which will interact with CS and promote the production of nanoparticles
 346 in the media.(Hong et al., 2014; Patel, Parikh, & Aboti, 2013; Luo, Zhang, Cheng, & Wang, 2010; Bugnicourt,
 347 Alcouffe, & Ladavière. 2014). On the other hand, stirring time does not show any effect on the particle size.
 348 Although it was reported in literature that stirring speed affected the particle size as the increase in the
 349 speed resulted in smaller particle size, this could be based on the increase in homogenization speed results
 350 in smaller particles (Hong,et al., 2014; Bugnicourt, Alcouffe, & Ladavière. 2014 ; Patel, Parikh, & Aboti, 2013).

351

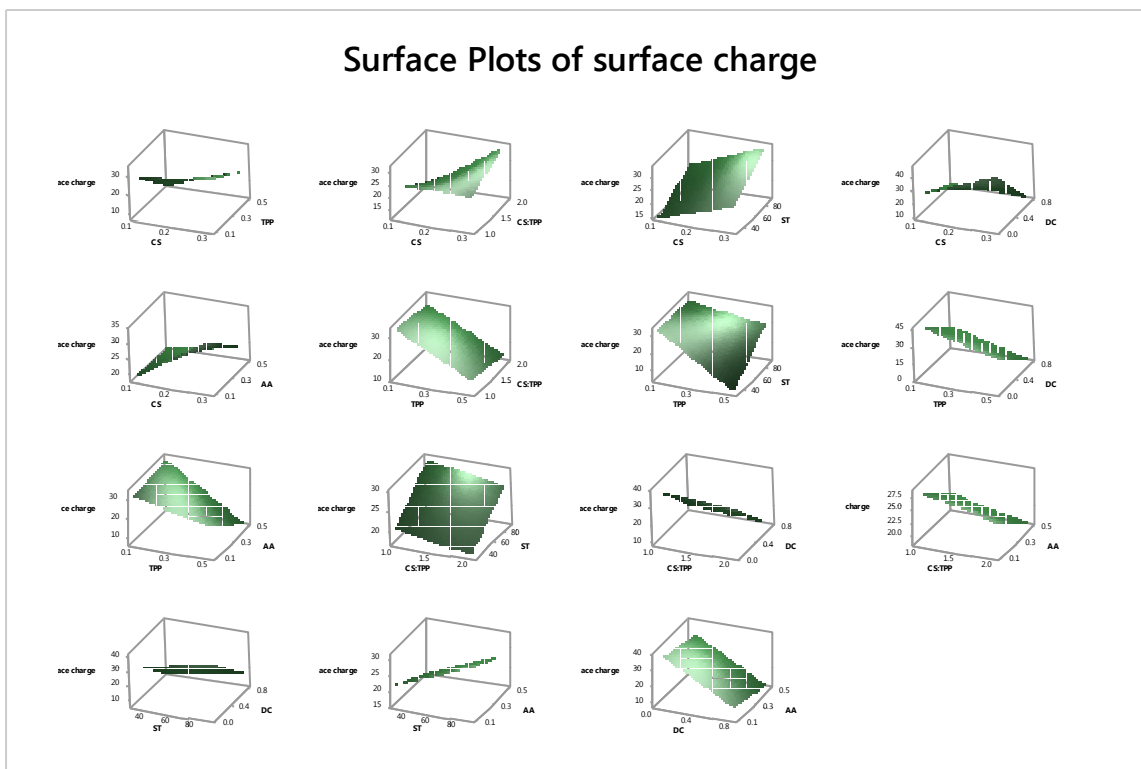
352 **3.1.2. The effect of different parameters on surface charge (zeta potential)**

353 The presence of glucosamine group on CS backbone contributes to the creation of positive charge on the
354 surface of the polymer in acidic solutions. CS positively charged surface plays an important role in improving
355 drug targeting and mucoadhesion properties. CS nanoparticles' surface charge was affected by most of the
356 variables, but it was clearly shown in the plot that the CS, TPP and drug concentration were the main factors
357 influenced the change of surface charge (Fig 5& 6).



358

359 Fig 5:- Main effects plot showing the influence of the independent variables on CS surface charge.



360

361 *Fig 6:- Response surface plots of interaction effects between different variables and their effect on CS surface*
 362 *charge. Hold values are 0.20 for CS, 0.30 for TPP, 1.50 for CS:TPP, 60.00 for ST, 0.45 for DC and 0.30 for AA.*

363 The increase in CS concentration will be accompanied with an increase in protonized $-NH_3^+$ which increases
 364 the positive charge on the surface of the nanoparticles (Hong et al., 2014; Patel, Parikh, & Aboti, 2013; Luo,
 365 Zhang, Cheng, & Wang, 2010; Bugnicourt, Alcouffe, & Ladavière. 2014). Contrariwise, increasing TPP
 366 concentration will increase the interaction between CS and TPP and reduce the overall surface charge on the
 367 particles due to the presence of the negative charge on the surface. In addition, the increase in the drug
 368 concentration resulted in a drop in zeta potential, which can be explained by the competition between CS
 369 and the drug to bind to TPP. Acetic acid did not have a significant effect (Fig 5), as it did not have a dramatic
 370 effect on the pH, all samples had a pH range of (pH 3.3-3.6).

371

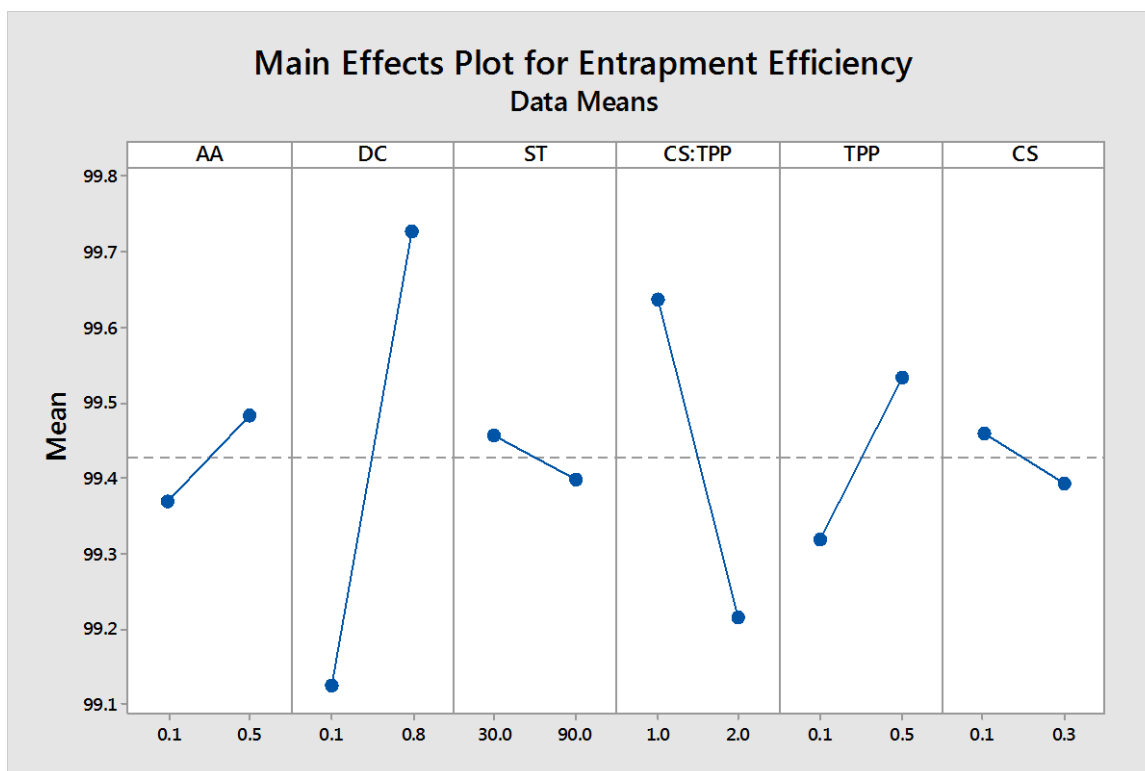
372 **3.1.3. The effect of different parameters had on encapsulated efficiency**

373

374 The encapsulated efficiency was detected by measuring the amount of drug (PMZ) in the supernatant, after
 375 centrifugation of the nanoparticles. The current study looked at 2 concentrations of PMZ; 0.4mg/ml,
 376 0.8mg/ml and the results obtained indicated an EE range of (95-99%).

377 The obtained results outlined that EE was significantly affected by the CS:TPP ratio and drug concentration
 378 (Figs 7&8). Increasing DC was associated with increasing the entrapment efficiency. Nonetheless, all the
 379 prepared formulations had entrapment efficiency greater than 95%. Previous studies had demonstrated that
 380 the nature of the drug -whether hydrophilic or hydrophobic- will not have an effect on the encapsulation
 381 efficiency (Cafaggi, et al., 2007; Bugnicourt, Alcouffe, & Ladavière. 2014; Klancke 2003). Moreover, the study
 382 conducted by Yan Wu et al., claimed that the drug concentration has no effect on the EE despite using
 383 similar concentration range (0.2-0.8mg/ml) to our study (Wu, Yang, Wang, Hu, & Fu, 2005)

384 There is a debate on the effect of CS concentration on EE of CS nanoparticles, previous studies conducted by
 385 Vandenberg et al., 2001 and Hassani 2014 reported that the increase in CS lead to the increase in drug
 386 encapsulation, mainly due to an increase in the CS concentration leading to an increase in the ion gelation
 387 hence better entrapment efficiency. In contrast a study by Wu et al. 2005 indicated that the increase of CS
 388 decreases the EE (Wu, Yang, Wang, Hu, & Fu, 2005). Nevertheless, our study demonstrated that CS
 389 concentration has no significant effect on PMZ entrapment ($p < 0.05$).

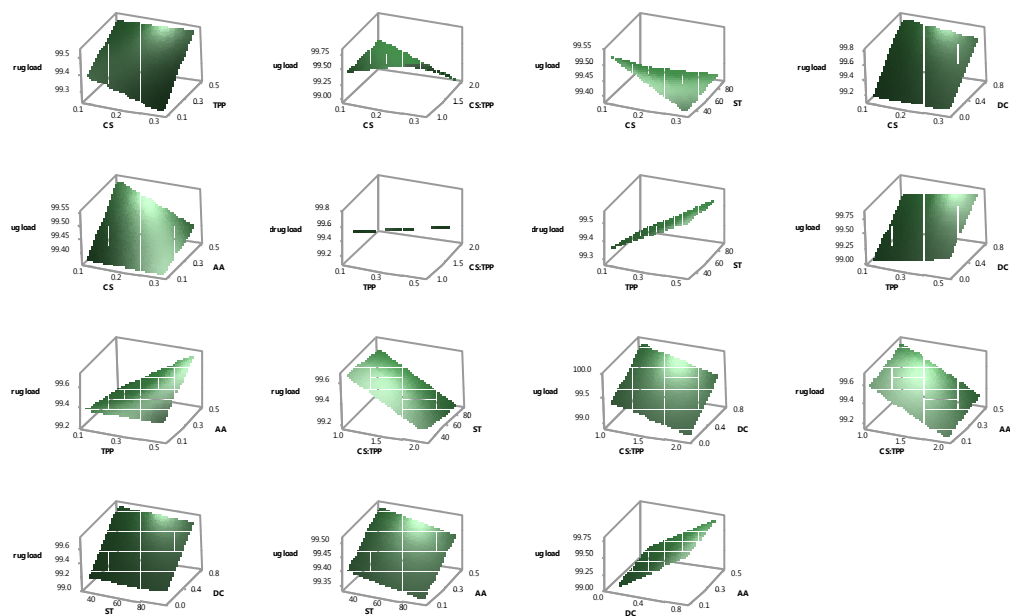


390

391 *Fig 7:- Main effects plot showing the influence of the independent variables on the entrapment efficiency of*
 392 *PMZ*

393

Surface Plots of Entrapment Efficiency



394

395 Fig 8:- Response surface plots of interaction effects between different variables and their effect on the
 396 entrapment efficiency of PMZ. Hold values are 0.20 for CS, 0.30 for TPP, 1.50 for CS:TPP, 60.00 for ST, 0.45
 397 for DC and 0.30 for AA.

398

399 After identifying the effect variables on the responses, an optimization study was performed by Minitab
 400 (Table 2), to determine the optimum conditions to produce the nanoparticles with maximum drug loading
 401 and targeted particle size of 250 nm. Nanoparticles were prepared using the optimal conditions and
 402 evaluated to determine the accuracy of the conditions produced; the results obtained from the sample
 403 showed a particle size of 280nm, with EE of 99% and zeta potential of 20.8 mV. Where Minitab predicted a
 404 particle size of 250nm and EE of 94%, this can clearly conclude the precision of the optimization study by
 405 Minitab.

406 *Table 2:- Summary of the optimised conditions for preparing CS-nanoparticles*

Concentration of CS	Concentration of TPP	CS:TPP	Concentration of PMZ	Concentration of acetic acid	Stirring time
0.1%	1%	5:2	0.8mg/ml	1%	90min

407

408 3.2. Characterisation of coated CS nanoparticles

409 The fast advances of polymeric sciences led to the introduction of a number of new polymers into the
 410 pharmaceutical industry and resulted into the production of a number of novel sustained release drug
 411 delivery systems. After optimisation of chitosan nanoparticles using the DOE approach, the optimised
 412 nanoparticulate system was coated with three polymers namely; PVP, PEG and PEAA which have cationic,

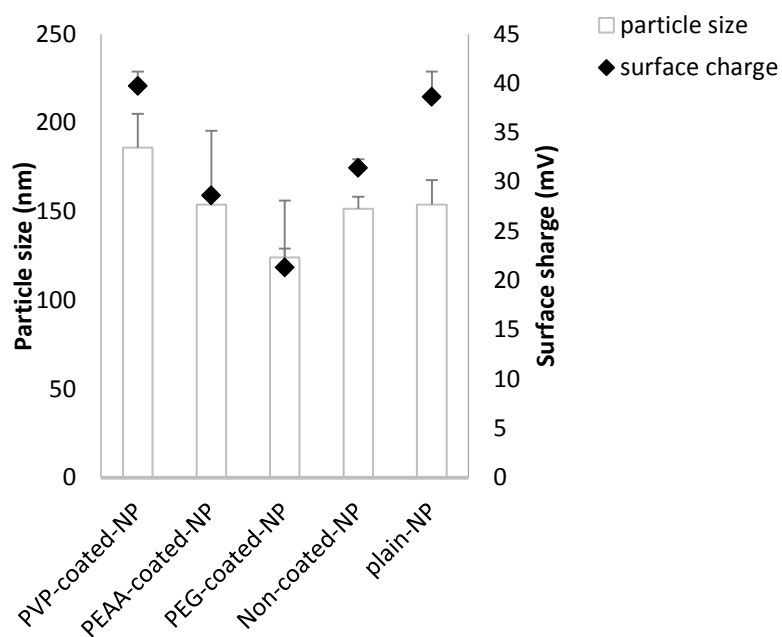
413 non-ionic and anionic nature, respectively. The nature of the coating polymer might affect the surface
 414 charge, particles size and loading capacity of chitosan nanoparticulate system. Both PVP (Park 2003) and
 415 PEG (Park 2001) were co-grafted with chitosan to improve the low solubility of the hydrophobic polymer in
 416 aqueous solutions. The new grafted polymers were used for delivery of DNA molecules and showed
 417 responsiveness (Park 2001; Park 2003). The particles size for non-coated CS nanoparticles was not affected
 418 ($p>0.05$) by the incorporation of PMZ (Fig 9 and Table 3). Non-coated particles showed particle size of
 419 151.4 ± 6.9 nm to 153.8 ± 14.0 nm for non-coated PMZ nanoparticles and PMZ-free nanoparticles respectively.
 420 Nonetheless, incorporation of the coating polymers during the manufacturing of CS nanoparticles has
 421 affected both the particles size and surface charge (Fig 9). Addition of PVP was associated with an increase
 422 ($p<0.05$) in the particle size which reached 186 ± 19 nm. The cationic nature of PVP might be the reason of
 423 increasing the particle size of CS nanoparticles as the polymer might compete with chitosan to interact with
 424 TPP during the manufacturing process which will reduce the ionic gelation capacity of chitosan ,therefore
 425 larger particles were formed. On the other hand, addition of PEG decreased the size of the particles
 426 prepared ($p<0.05$). This can be explained by the ability of the electronegative oxygen atom of PEG to form
 427 intramolecular hydrogen bonding with the electropositive amino hydrogen on CS as reported by (Kim and
 428 Lee, 1995) which in turn tighten the nanoparticle structure, therefore a smaller size (124 ± 5.2 nm; PDI
 429 0.32 ± 0.04) was obtained. In a similar pattern, the surface charge on PEG-CS coated nanoparticles has
 430 decreased significantly ($p<0.05$) to 21.3 ± 6.8 mV when compared to non-coated PMZ nanoparticles (31.4 ± 0.9
 431 mV). Similar trend was reported by Wu et al (2005) and Quellec et al., (1998). PEAA is the third polymer used
 432 to coat CS nanoparticles. PEAA did not have any effect on the particle size ($p>0.05$) or the surface charge of
 433 the prepared nanoparticulate system (Fig 9). This could be attributed to the weak acidic nature of the
 434 polymer (pKa of 4.25) which has a minimal effect on the pH of CS acetic acid solution and hence minimal
 435 effect on the characteristics of the nanoparticles as suggested by (Wu, Yang, Wang, Hu, & Fu, 2005;
 436 Bugnicourt, Alcouffe, & Ladavière. 2014; Quellec et al., 1998.)

437 *Table 3:- Summary of particle size, surface charge, PDI and entrapment efficiency of coated and non-coated*
 438 *CS-nanoparticles (mean±SD)*

Sample	particle size (nm)	surface charge (mV)	PDI	EE%
PVP-coated nanoparticle	186±19.00	39.7±1.50	0.27±0.19	99.69±0.04
PEAA-coated nanoparticle	153.8±5.40	28.6±6.60	0.47±0.10	99.74±0.00
PEG-coated nanoparticle	124±5.20	21.3±6.80	0.32±0.04	99.77±0.06
Non-coated PMZ nanoparticles	151.4±6.90	31.4±0.90	0.67±0.08	99.77±0.06
PMZ-free nanoparticles	153.8±14.00	38.6±2.60	0.42±0.29	-

439

440



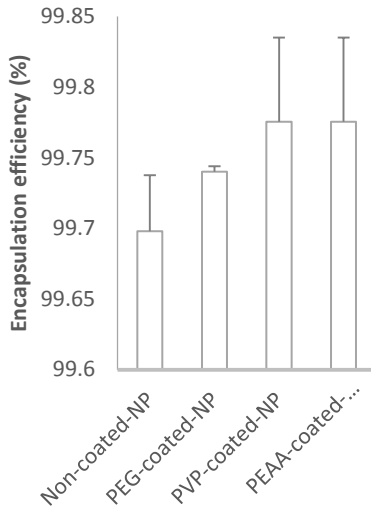
441

442 *Fig 9:- Effect of coating polymers on the particle size and surface charge of CS nanoparticles.*

443

444 Encapsulation efficiencies (EE) of coated nanoparticles were evaluated as well (Fig 10). All coated
445 nanoparticulate systems showed high percentage of EE ranged around (99.5%-99.9%), which suggest that
446 different coating polymers did not affect the encapsulation efficiency of CS nanoparticles ($p>0.05$).

447



449

450 *Fig 10:-Effect of coating polymers on the encapsulation efficiency of CS nanoparticles.*

451 **3.3. Scanning electron microscopy (SEM)**

452

453 In order to investigate the morphology and surface properties of the prepared nanoparticles, SEM was used.
 454 (Fig11) shows SEM images of PMZ HCl, chitosan polymer, plain CS-nanoparticles, PEG-coated nanoparticles,
 455 PVP-coated nanoparticles, PEAA-coated nanoparticles and non-coated CS nanoparticles. PMZ HCl showed
 456 cubic crystals with a wide range of particle size ranging from few μms to $200 \mu\text{m}$. Small and large crystals
 457 aggregate together forming raspberry like aggregates (Fig11B). Chitosan particles were irregular in shape
 458 with some folds on their surface. CS particles showed large particle size greater than $400 \mu\text{m}$ (Fig 11C). All
 459 the prepared nanoparticles; coated and non-coated were spherical in shape and showed particles size in
 460 nano-range as suggested by DLS studies. Plain CS-nanoparticles showed a smooth surface without any
 461 evidence of aggregate formation; probably the high surface charge ($\xi=38.6\pm 2.6 \text{ mV}$) prevented any
 462 aggregation through electrostatic repulsion between the positively charge particles. Similarly, only few
 463 aggregates were observed when nanoparticles were coated with PVP (Fig11F). In contrary, loads of
 464 aggregates appeared under the microscope when PEAA was used as a coating polymer (Fig11G), this could
 465 be attributed to the anionic nature of PEAA which decreased the overall charge on the CS nanoparticles
 466 ($\xi=28.6\pm 6.6 \text{ mV}$). Similar trend was observed with PEG-coated nanoparticles (Fig 11E).

467

468

469

470

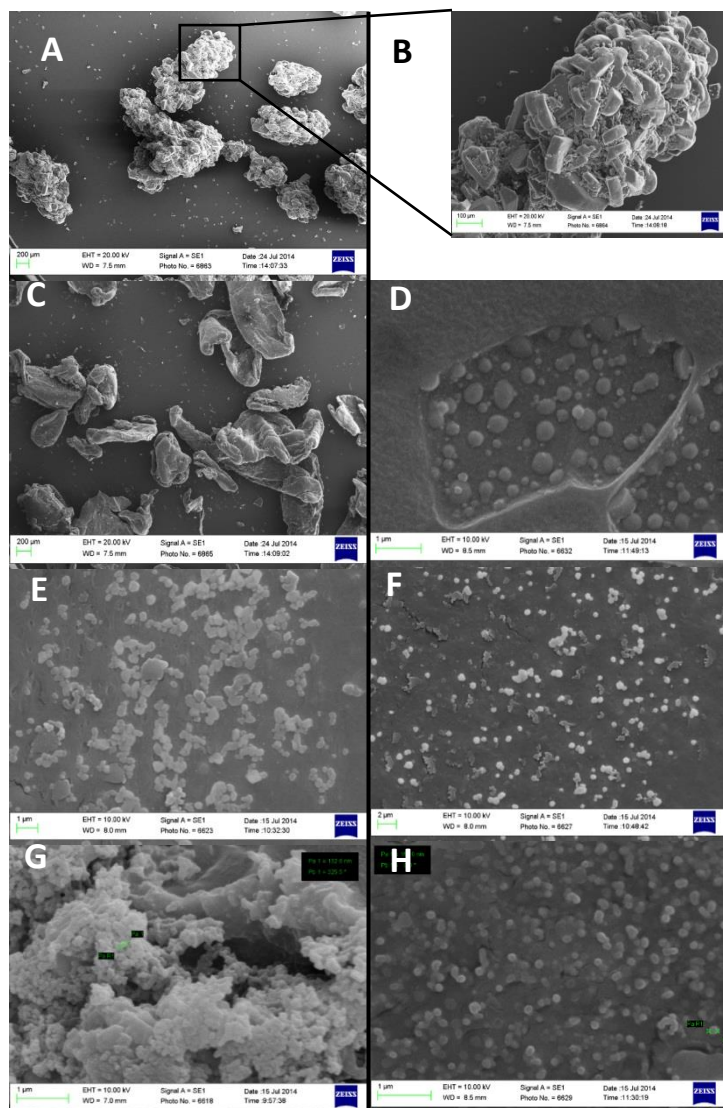
471

472

473

474

475
476
477
478
479
480
481
482
483
484
485
486
487
488
489
490
491
492
493
494



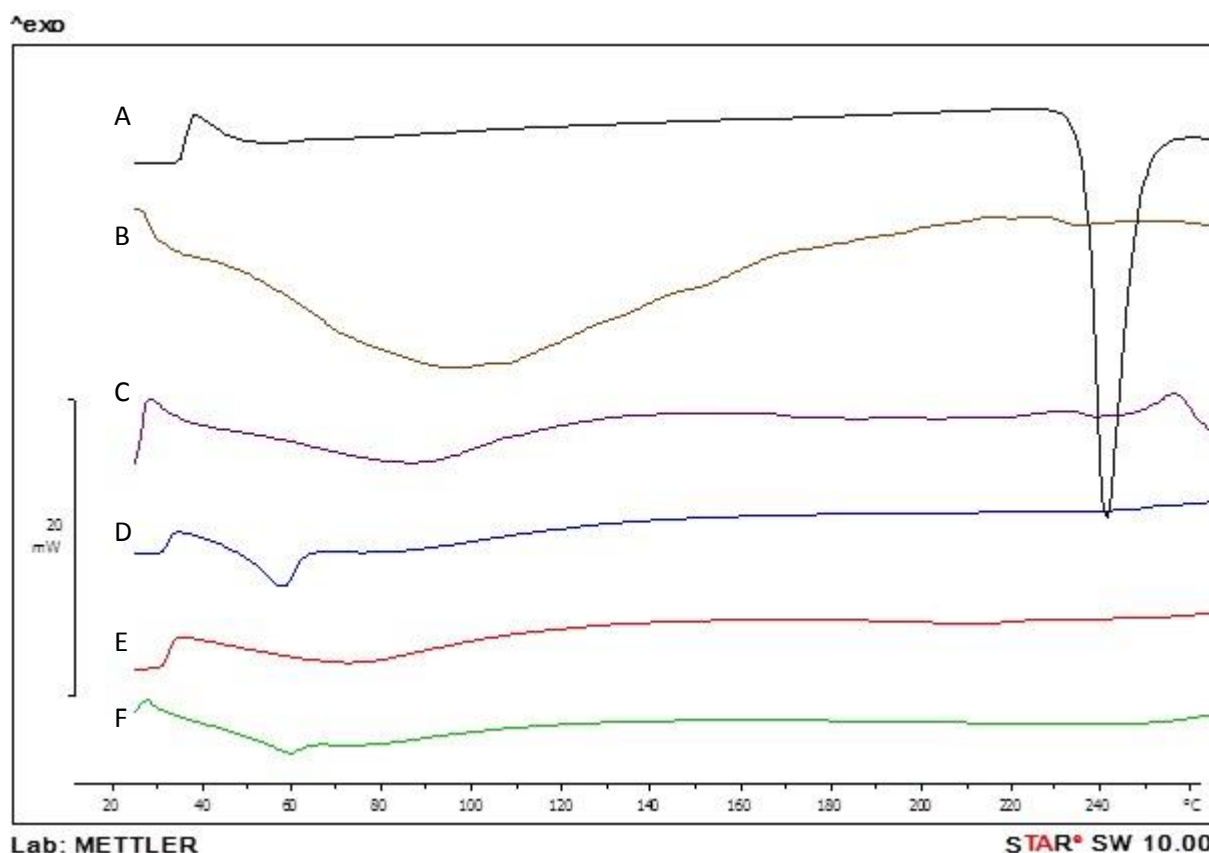
495 *Fig 11:- SEM images of PMZ HCl at low magnification (A) and high magnification (B), chitosan polymer (C), plain CS-nanoparticles (D),*
496 *PEG-coated nanoparticles (E), PVP-coated nanoparticles (F), PEAA-coated nanoparticles (G) and non-coated CS nanoparticles (H).*

497
498
499

3.4. Thermal analysis

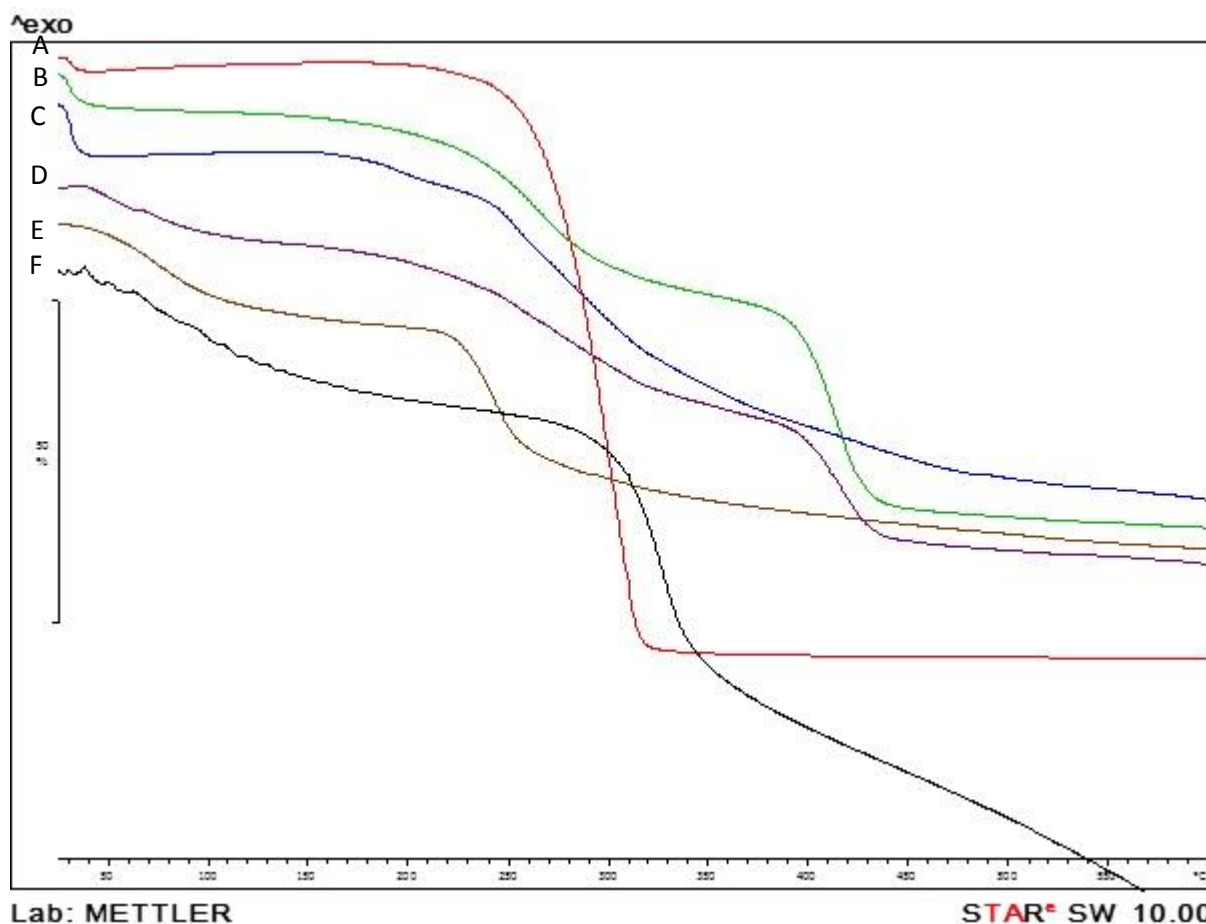
500 Differential scanning calorimeter is used to determine any change in the physic-chemical properties of the
501 material by measuring the energy transfer from and to PMZ. Moreover, differential scanning calorimetry will
502 enable investigation of any interaction between PMZ and CS or the coating polymers used in this study.

503 (Fig12) shows the rate of heat absorption for PMZ, CS, PEG-coated nanoparticles, PVP-coated nanoparticles,
504 PEAA-coated nanoparticles and non-coated CS nanoparticles. DSC has shown a sharp endothermic peak at
505 234 °C corresponding to the melting of PMZ HCl salt (Fig12A) (Lutka, A 2002; Ambrogi, Nocchetti, & Latterini,
506 2014). Chitosan thermal scans has shown a broad endothermic peak between 60 and 140 °C and this is
507 attributed to evaporation of water that is associated with the hydrophilic groups of CS (Figure 12 B).
508 Coupling DSC scans with TGA can confirm this finding as a weight loss of (19 %) was observed between 60-
509 140 °C (Fig13B). Similar findings were reported earlier by (Dong, Ruan, Wang, Zhao, & Bi, 2004; Mladenovska
510 et al., 2007). PMZ-CS nanoparticles (Fig12F) did not show any endothermic or exothermic peaks and PMZ HCl
511 endothermic peak disappeared which suggests possible interaction between the drug and CS by Van der
512 Waals force within the nanoparticles. Moreover, it was reported that spaces between CS chain provide
513 favourable conditions for dispersing drug within CS nanoparticles (Sarmiento, Ferreira, Veiga, & Ribeiro,
514 2006; Dos et al., 2011)



515

516 Fig 12:- DSC scans of PMZ HCl salt (A), CS (B), PEG-coated nanoparticles (C), PVP-coated nanoparticles (D), PEAA-coated nanoparticles
517 (E) and non-coated CS nanoparticles (F).



518

519 *Fig 13:- TGA scans of PMZ HCl salt (A), PEAA-coated nanoparticles (B), non-coated CS nanoparticle (C), PVP-coated nanoparticles (D)*
 520 *PEG-coated CS nanoparticles (E) and non-coated CS nanoparticles (F).*

521 CS-coated nanoparticles showed similar scans to non-coated CS-nanoparticles as PMZ HCl endothermic peak
 522 disappeared because of the dispersion of the drug between CS and the coating polymer used.

523 3.5. ODTs preparation and evaluation

524

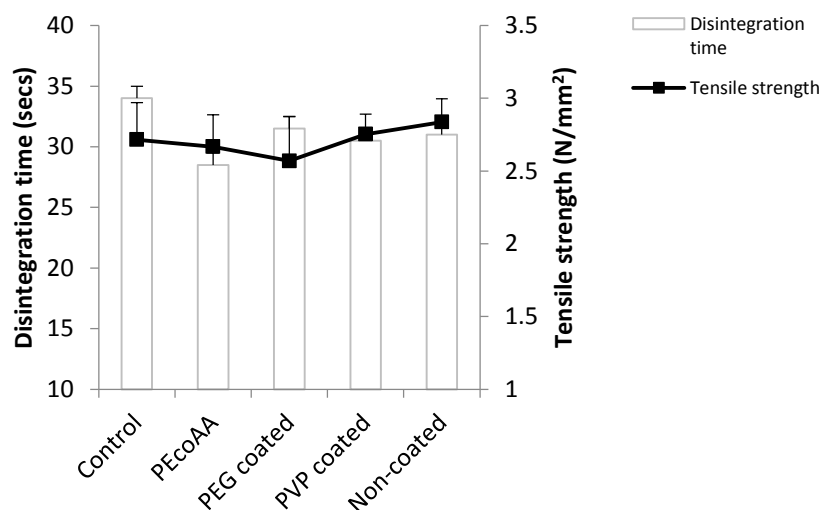
525 After preparation and characterisation of various CS-nanoparticles, the particles were incorporated into
 526 orally disintegrating tablet matrix adapted from (ElShaer, A, Butt, U, Rauf, I , Sohaib Saboley, & Gawad, M
 527 2014) and based on the following formulation 25% LH-B1, 1% Magnesium stearate, 5% PMZ and 69% D (+)-
 528 Lactose Monohydrate. After the preparation of ODTs, the tablets were then evaluated for their hardness,
 529 friability, disintegration time, dissolution profiles.

530 3.5.1. Hardness, disintegration time and friability

531

532 Hardness and friability tests were performed to determine if the tablets produced have a significant
 533 mechanical strength to stand fraction and erosion. The mechanical strength of ODTs is a critical parameter,
 534 as ODTs are prepared under low compression in order to form highly porous compress for fast
 535 disintegration. Nonetheless, the preparation process together with the excipients used might results in
 536 producing a friable/ brittle tablet. Control ODTs did not contain any nanoparticles within their matrix and
 537 showed fast disintegration time of 34 ± 1.4 sec and high tensile strength of 2.7 ± 0.25 N/mm². Addition of

538 coated and non-coated CS nanoparticles into ODTs tablet matrix did not distort the characteristics of the
 539 tablets (Fig 14) and Table (4). All ODTs showed disintegration time between 25- 35 sec and tensile strength
 540 ranging from 2.5-3 N/mm². All tablets showed no significant effect ($p < 0.05$) in disintegration time comparing
 541 to each other ($p > 0.05$), but had a statistical significant affect comparing to the disintegration time of the
 542 control tablet ($p < 0.05$). All the prepared tablets passed the friability test (Table 4) with highest friability of
 543 0.9% exhibited by ODTs containing PVP coated nanoparticles.



544

545 Fig 14:- Tensile strength and disintegration time of ODTs containing non-coated CS-nanoparticles, PEAA coated CS-nanoparticles, PEG
 546 coated CS nanoparticles, PVP coated CS nanoparticles and control ODTs.

547 Table 4:- Thickness, diameter (mean±SD) and friability of ODTs tablets containing coated and non-coated CS nanoparticles.

sample	Thickness (mm)	Diameter (mm)	Friability (%)
Control tablet	13.1±0.04	2.71±0.25	0.75%
PEAA coated nanoparticle tablet	13.02±0.04	2.66±0.22	0.5%
PEG coated nanoparticle tablet	13±0	2.56±0.30	0.7%
PVP coated nanoparticle tablet	13.06±0.054	2.66±0.05	0.9%
Non-coated nanoparticle tablet	13.04±0.054	2.68±0.04	0.6%

548

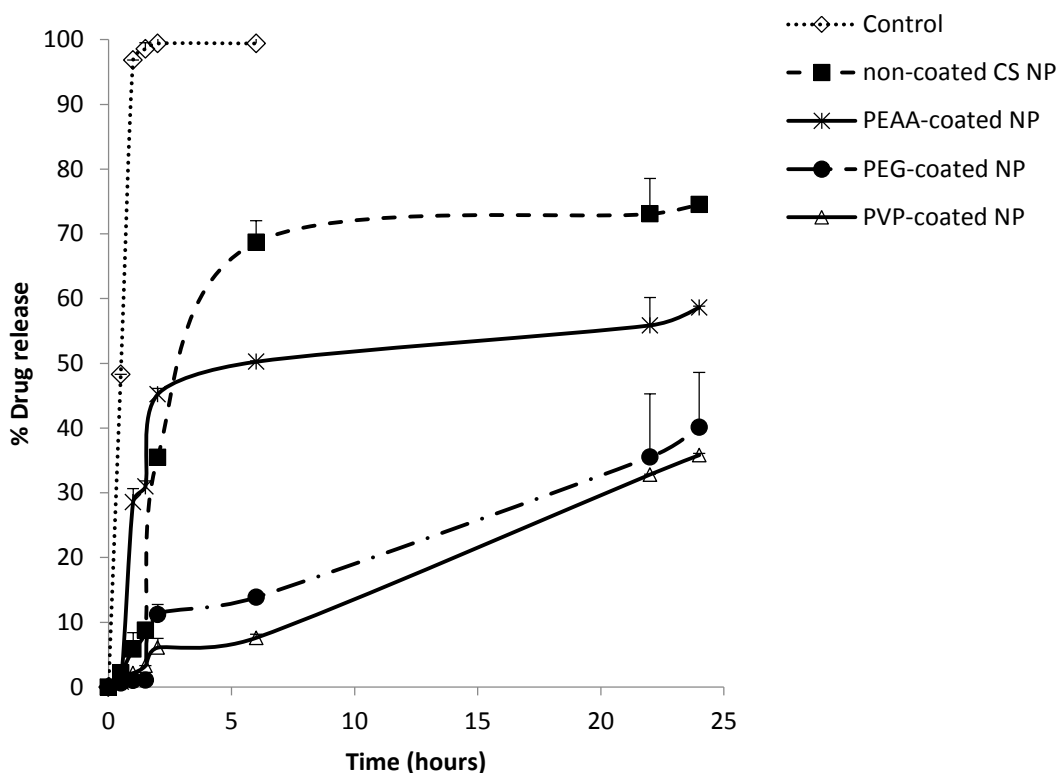
549 3.5.2. Dissolution test

550

551 In order to evaluate the release profile across CS-nanoparticles containing tablets, *in vitro* dissolution studies
 552 were performed. Control tablets showed a fast release of PMZ as 46.1±0.3 % of the drug was released
 553 within 20 mins of the dissolution study and 97.3±0.13% was released at 60 mins. On the other hand, tablets
 554 containing CS-nanoparticles showed a slower release profile that became even slower upon coating the
 555 nanoparticles (Fig15). Non-coated chitosan nanoparticles managed to sustain the drug release for 24 hours
 556 with only 35.5±0.14% and 68.8±3.3% after 2 and 6 hours respectively. Similar release profiles were reported

557 by (Lu et al., 2009) when using CS nanoparticles to deliver aminoglycosides such as gentamicin and
558 tobramycin. As more than 60% of the drugs were retained inside CS nanoparticles for 6 hours at pH of 1.2.
559 Unmodified CS has been used intensively to sustain the drug release for several therapeutic agents such as
560 ammonium glycyrrhizinate. (Wu, Yang, Wang, Hu, & Fu, 2005) dorzolamide hydrochloride, and pramipexole
561 hydrochloride (Papadimitriou, Bikiaris, Avgoustakis, Karavas, & Georgarakis, 2008) ciprofloxacin (Jain, &
562 Banerjee, 2008) and even for peptides and proteins (Jiang, Pan, Cao, Jiang, Hua, & Zhu, 2012).
563 Nevertheless, CS-nanoparticles fail to sustain the drug release for longer time as the acidic conditions in the
564 stomach solubilise chitosan (George, & Abraham, 2006). Therefore a second coating polymer was used in
565 this study. The *in vitro* dissolution test indicated that coated nanoparticles had a slower release profile
566 compared to non-coated, even after 24hr the drug release from the nanoparticle was not complete Fig (15).

567 PEAA coated nanoparticles showed a burst effect as 45 ± 0.9 % of PMZ was release within 2 hours of the
568 dissolution study and the drug release remained below $58.6\pm 0.23\%$ during the time course of the
569 experiment. Despite the weak acidic nature of PEAA which was believed to reduce its dissolution under the
570 acidic conditions of this study (0.1N HCl), PEAA-CS particles exhibited a burst effect, possibly because some
571 of PMZ was attached to the surface of the nanoparticles and released ring the first few hours of the
572 dissolution study as suggested earlier by (Patel, Parikh, & Aboti, 2013). On the other hand, PVP and PEG
573 coated nanoparticles showed the slowest amount of drug release over 24hr. PEG and PVP-coated CS
574 nanoparticles released $13.86\pm 0.13\%$ and 7.6 ± 0.54 % after 6 hours of the dissolution study respectively. And
575 less than 45% of PMZ after 24 hours of the dissolution study.

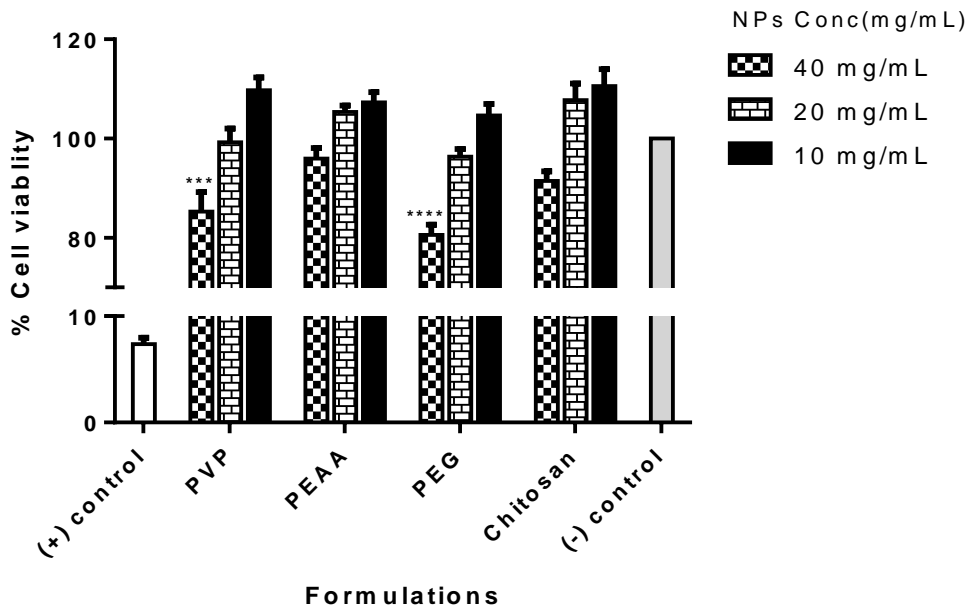


576

577 Fig 15:- In vitro dissolution study of orally disintegrating tablets containing PMZ (control), non-coated CS NPs, PEAA-coated CS-NPs,
 578 PEG-coated CS-NPs and PVP-coated CS-NPs.

579 **3.5.2.3. Sulforhodamine B (SRB) cytotoxic assay.**

580 The SRB assay was used to study the cytotoxic effect of the prepared nanoparticles. Figure (16) illustrate the
 581 cell viability of Caco-2 cell lines after 24 hours incubation with different concentration of the nanoparticles
 582 compared to the negative control. The average cell viability for the highest concentration (40 mg/mL) of the
 583 PVP coated nanoparticles was 85% ($p < 0.05$) compared to the untreated cell (negative control), similar
 584 findings were suggested earlier by Lara et al (2010). Likewise, the cell viability of PEG coated nanoparticles
 585 were significantly ($p < 0.05$) reduced to 80%, this could be ascribed to the ability of PEG to form hydrogen
 586 bonding with surrounding water which in turn increases the osmotic pressure of the surrounding media. This
 587 osmotic shock will be associated with disorganisation of the nuclear chromatin cells of the Caco-2 cells by
 588 hyper-condensation of the nuclear chromatin and accumulation of cytoplasmic vesicles as suggested by
 589 Gilles et al., 1995 and Parnaud et al., 2001. On the other hand, lower concentrations of both PVP and PEG
 590 (20 mg/mL and 10 mg/mL) showed no signs of toxicity on the mammalian cells (Fig 16). In contract to PVP
 591 and PEG behaviors, 40 mg/mL of the chitosan and PEAA nanoparticles had no significant ($p > 0.05$) effect on
 592 the cells' viability. The average cell viability for the chitosan and PEAA coated nanoparticles were 92% and
 593 96% respectively. These results are in agreement with previous studies conducted by (Huang et al., 2004)
 594 suggesting that higher concentrations of CS is associated with cell toxicity because of the higher surface
 595 charge density which is a high contributor to cell death. Other concentration of the prepared nanoparticles
 596 had no significant effect on the Caco-2 cell lines after 24 hours incubation period ($p > 0.05$)



597

598 *Figure 16:- SRB cytotoxic assay for the effect of chitosan and coated nanoparticles on Caco-2 cell line after 24 hours incubation.*
 599 *Results express as mean value \pm SD (n=6), ***p<0.001, ****p<0.0001*

600

601 **Conclusion**

602

603 The properties of CS nanoparticles was engineered using Minitab in order to manufacture a new formulation
 604 of SR-ODTs. Minitab studies revealed that the nanoparticles' particle size is affected by most of the
 605 independent variables. The concentration of TPP and CS was associated with an increase in the particles size
 606 and this is possibly due to the stiffening of the cross linking bonds between TPP and CS, and the increase in
 607 the viscosity which will affect the shear capacity of homogenization leading to the formation of aggregates
 608 with large particle size, respectively. Drug concentration and CS:TPP ratios were the two main variables
 609 affecting the encapsulations efficiency. The engineered nanoparticles were further characterised using SEM
 610 which revealed that all the samples were spherical in shape with smooth surface and had particle size
 611 ranging between 100- 200 nm that goes in line with DLS results. Optimised CS-nanoparticles were further
 612 coated with polyvinylpyrrolidone (PVP), polyethylene glycol (PEG) and polyethylene co-acrylic acid (PEAA). The
 613 coated nanoparticles were incorporated into ODTs. All tablets had passed the friability test and showed good
 614 tensile strength despite disintegrating in less than 40sec. The drug release profile was studied in 0.01M HCL
 615 solution showing that tablets containing PVP and PEG coated nanoparticles managed to sustain the drug
 616 release over 24hr, yet showed a slight toxic effect on Caca-2 cell lines at high concentrations of 40 mg/mL.
 617 On the other hand, non-coated and PEAA nanoparticles showed a faster rate of release without any
 618 pronounced effect on the viability of Caco-2 cells.

619

620

621 **Conflict of Interest:**

622 Authors declare that there is no conflict of interest.

623

624 **Acknowledgement**

625 Authors would like to thank Dr. Siamak Soltani-Khankahdani and Mr Richard Giddens for their technical help
626 and support during the project.

627

628 **References**

- 629 Abbaspour, M. R., Sadeghi, F., & Garekani, H. A. (2008). Design and study of ibuprofen disintegrating
630 sustained-release tablets comprising coated pellets. *European Journal of Pharmaceutics and*
631 *Biopharmaceutics*, 68(3), 747-759.
- 632 Abdelbary A., El-Gendy N., Hosny A. (2012). Microencapsulation approach for orally extended delivery of
633 glipizide: In vitro and in vivo evaluation. *Indian journal of pharmaceutical sciences*, 74 (4), 319.
- 634 Abdul, S., & Poddar, S. S. (2004). A flexible technology for modified release of drugs: multi layered tablets.
635 *Journal of controlled release*, 97(3), 393-405.
- 636 Ambrogi, V., Nocchetti, M., & Latterini, L. (2014). Promethazine–Montmorillonite Inclusion Complex To
637 Enhance Drug Photostability. *Langmuir*, 30(48), 14612-14620.
- 638 Beckert TE, Lehmann K, & Schmidt PC. (1996) Compression of enteric-coated pellets to disintegrating tablets.
639 *Int J Pharm*, 143(1) pp 13-23.
- 640 Bugnicourt, L., Alcouffe, P., & Ladavière, C. (2014). Elaboration of chitosan nanoparticles: Favorable impact of
641 a mild thermal treatment to obtain finely divided, spherical, and colloidally stable objects. *Colloids and*
642 *Surfaces A: Physicochemical and Engineering Aspects*, 457, 476-486.
- 643 Cafaggi, S., Russo, E., Stefani, R., Leardi, R., Caviglioli, G., Parodi, B., & Viale, M. (2007). Preparation and
644 evaluation of nanoparticles made of chitosan or N-trimethyl chitosan and a cisplatin–alginate complex.
645 *Journal of Controlled Release*, 121(1), 110-123.
- 646 Calvo, P., Remunan-Lopez, C., Vila-Jato, J. L., & Alonso, M. J. (1997). Novel hydrophilic chitosan-polyethylene
647 oxide nanoparticles as protein carriers. *Journal of Applied Polymer Science*, 63(1), 125-132.
- 648 Dodov, M. G., Calis, S., Crcarevska, M. S., Geskovski, N., Petrovska, V., & Goracinova, K. (2009). Wheat germ
649 agglutinin-conjugated chitosan–Ca–alginate microparticles for local colon delivery of 5-FU: Development and
650 in vitro characterization. *International journal of pharmaceutics*, 381(2), pp 166-175.
- 651 Dong, Y., Ruan, Y., Wang, H., Zhao, Y., & Bi, D. (2004). Studies on glass transition temperature of chitosan
652 with four techniques. *Journal of Applied Polymer Science*, 93(4), 1553-1558.
- 653 Dos Santos Silva, M., Cocenza, D. S., Grillo, R., de Melo, N. F. S., Tonello, P. S., de Oliveira, L. C., ... & Fraceto,
654 L. F. (2011). Paraquat-loaded alginate/chitosan nanoparticles: Preparation, characterization and soil sorption
655 studies. *Journal of hazardous materials*, 190(1), 366-374.
- 656 ElShaer A, Butt U, Rauf I, & Saboley S. (2014) Mess Gawad: Multi-stage Strategy to Optimize the Formulation
657 of Directly Compressed Orally Disintegrating Tablets., AAPS., San Diego, USA. November 2014
658 <https://2014aapsam.zerista.com/poster/member/24071> (Accessed on 22/12/2014)
- 659 Ford, J. L., Rubinstein, M. H., & Hogan, J. E. (1985). Formulation of sustained release promethazine
660 hydrochloride tablets using hydroxypropyl-methylcellulose matrices. *International journal of pharmaceutics*,
661 24(2), 327-338.
- 662 Fulzele, S., Moe, D., & Hamed, E. (2012). ODT TECHNOLOGY-Lyoc (Lyophilized Wafer): An Orally
663 Disintegrating Tablet Technology. *Drug Dev Del*, 1-5.

664 George, M., & Abraham, T. E. (2006). Polyionic hydrocolloids for the intestinal delivery of protein drugs:
665 alginate and chitosan—a review. *Journal of controlled release*, 114(1), 1-14.

666 Gilles, R., Belkhir, M., Compere, P., Liboulle, C. and Thiry, M. (1995). Effect of high osmolarity acclimation on
667 tolerance to hyperosmotic shocks in L929 cultured cells. *Tissue and Cell* , 27 , 679- 687.

668 Gokhale, A., & Sundararajan, P. ORALLY DISINTEGRATING TABLETS-Novel Controlled Release Formulation for
669 Orally Disintegrating Tablets Using Ion Exchange Resins. *drug Development & Delivery.*, 13 ,5

670 Gryczke, A., Schminke, S., Maniruzzaman, M., Beck, J., & Douroumis, D. (2011). Development and evaluation
671 of orally disintegrating tablets (ODTs) containing Ibuprofen granules prepared by hot melt extrusion. *Colloids
672 and Surfaces B: Biointerfaces*, 86(2), 275-284.

673 Hassani N. A., Abdouss, M., Faghihi, S. (2014). Synthesis and evaluation of PEG-O-chitosan nanoparticles for
674 delivery of poor water soluble drugs: Ibuprofen. *Materials Science and Engineering: C* 8, 1;41(0), 91-99.

675 Hirani, J. J., Rathod, D. A., & Vadalia, K. R. (2009). Orally disintegrating tablets: a review. *Tropical Journal of
676 Pharmaceutical Research*, 8(2).

677 Hong, W., Chen, D., Jia, L., Gu, J., Hu, H., Zhao, X., & Qiao, M. (2014). Thermo-and pH-responsive copolymers
678 based on PLGA-PEG-PLGA and poly (l-histidine): synthesis and in vitro characterization of copolymer micelles.
679 *Acta biomaterialia*, 10(3), 1259-1271.

680 Huang, M., Khor, E., Lim, L. (2004). Uptake and Cytotoxicity of Chitosan Molecules and Nanoparticles: Effects
681 of Molecular Weight and Degree of Deacetylation., *Pharmaceutical Research*. 21,(2), 344-354

682

683 Jain, D., & Banerjee, R. (2008). Comparison of ciprofloxacin hydrochloride-loaded protein, lipid, and chitosan
684 nanoparticles for drug delivery. *Journal of Biomedical Materials Research Part B: Applied Biomaterials*, 86(1),
685 105-112.

686 Jiang, J., Pan, X., Cao, J., Hua, D., & Zhu, X. (2012). Synthesis and property of chitosan graft copolymer by
687 RAFT polymerization with tosylic acid–chitosan complex. *International journal of biological macromolecules*,
688 50(3), 586-590.

689 Kaloti, M., & Bohidar, H. B. (2010). Kinetics of coacervation transition versus nanoparticle formation in
690 chitosan–sodium tripolyphosphate solutions. *Colloids and Surfaces B: Biointerfaces*, 81(1), 165-173.

691 Kavanagh, J. J., Grant, G. D., & Anoopkumar-Dukie, S. (2012). Low dosage promethazine and loratadine
692 negatively affect neuromotor function. *Clinical Neurophysiology*, 123(4), 780-786.

693 Kim, S.S., Lee, Y.M. (1995). Synthesis and properties of semiinterpenetrating polymer networks composed of -
694 chitin and poly(ethylene glycol). *Macromer. Polym.* 36, 4497–4501.

695 Klancke, J. (2003) Dissolution testing of orally disintegrating tablets. *Dissolution technologies*, 10(2), 6-9.

696 Kondo, K., Ito, N., Niwa, T., & Danjo, K. (2013). Design of sustained release fine particles using two-step
697 mechanical powder processing: Particle shape modification of drug crystals and dry particle coating with
698 polymer nanoparticle agglomerate. *International journal of pharmaceutics*, 453(2), 523-532.

699 Krause J, Breitzkreutz J. (2008) Improving drug delivery in paediatric medicine. *Pharm Med*,22(1), 41-50.

700 Lara, H.H., Ixtepan-Turrent, L., Garza-Treviño L.N., Rodriguez-Padilla, C. (2010). PVP-coated silver
701 nanoparticles block the transmission of cell-free and cell-associated HIV-1 in human cervical culture., *Journal*
702 *of Nanobiotechnology*, 8, (15).

703 Lindgren, S., Janzon, L. (1991). Prevalence of swallowing complaints and clinical findings among 50–79-year-
704 old men and women in an urban population. *Dysphagia*, 6(4), 187-192.

705 Li, F. Q., Yan, C., Bi, J., Lv, W. L., Ji, R. R., Chen, X., & Hu, J. H. (2011). A novel spray-dried nanoparticles-in-
706 microparticles system for formulating scopolamine hydrobromide into orally disintegrating tablets.
707 *International journal of nanomedicine*, 6, 897.

708 Li, P., Dai, Y. N., Zhang, J. P., Wang, A. Q., & Wei, Q. (2008). Chitosan-alginate nanoparticles as a novel drug
709 delivery system for nifedipine. *International journal of biomedical science: IJBS*, 4(3), 221.

710 Luo, Y., Zhang, B., Cheng, W. H., & Wang, Q. (2010). Preparation, characterization and evaluation of selenite-
711 loaded chitosan/TPP nanoparticles with or without zein coating. *Carbohydrate Polymers*, 82(3), 942-951.

712 Lu, E., Franzblau, S., Onyuksel, H., & Popescu, C. (2009). Preparation of aminoglycoside-loaded chitosan
713 nanoparticles using dextran sulphate as a counterion. *Journal of microencapsulation*, 26(4), 346-354.

714 Lutka, A. N. N. A. (2002). Investigation of interaction of promethazine with cyclodextrins. *Acta poloniae*
715 *pharmaceutica*, 59(1), 45-52.

716 Makhija, S. N., & Vavia, P. R. (2002). Once daily sustained release tablets of venlafaxine, a novel
717 antidepressant. *European journal of pharmaceutics and biopharmaceutics*, 54(1), 9-15.

718 Mladenovska, K., Cruaud, O., Richomme, P., Belamie, E., Raicki, R. S., Venier-Julienne, M. C., & Goracinova, K.
719 (2007). 5-ASA loaded chitosan–Ca–alginate microparticles: Preparation and physicochemical
720 characterization. *International Journal of Pharmaceutics*, 345(1), 59-69.

721 Najafabadi, A. H., Abdouss, M., & Faghihi, S. (2014). Synthesis and evaluation of PEG-O-chitosan
722 nanoparticles for delivery of poor water soluble drugs: Ibuprofen. *Materials Science and Engineering: C*, 41,
723 91-99.

724 Papadimitriou, S., Bikiaris, D., Avgoustakis, K., Karavas, E., & Georgarakis, M. (2008). Chitosan nanoparticles
725 loaded with dorzolamide and pramipexole. *Carbohydrate Polymers*, 73(1), 44-54.

726 Park, I. K., Kim, T. H., Park, Y. H., Shin, B. A., Choi, E. S., Chowdhury, E. H., ... & Cho, C. S. (2001).
727 Galactosylated chitosan-graft-poly (ethylene glycol) as hepatocyte-targeting DNA carrier. *Journal of*
728 *controlled release*, 76(3), 349-362.

729 Park, I. K., Ihm, J. E., Park, Y. H., Choi, Y. J., Kim, S. I., Kim, W. J., ... & Cho, C. S. (2003). Galactosylated chitosan
730 (GC)-graft-poly (vinyl pyrrolidone)(PVP) as hepatocyte-targeting DNA carrier: Preparation and
731 physicochemical characterization of GC-graft-PVP/DNA complex (1). *Journal of controlled release*, 86(2), 349-
732 359.

733 Patel, B. K., Parikh, R. H., & Aboti, P. S. (2013). Development of oral sustained release rifampicin loaded
734 chitosan nanoparticles by design of experiment. *Journal of drug delivery*, 2013.

735 Parnaud, G., Corpet, D. and Payrastra, L. (2001). Cytostatic effect of polyethylene-glycol on human colonic
736 adenocarcinoma cells., *Int. J. Cancer*: 92, 63-69.

737 Quellec, P., Gref, R., Perrin, L., Dellacherie, E., Sommer, F., Verbavatz, J. M., & Alonso, M. J. (1998). Protein
738 encapsulation within polyethylene glycol-coated nanospheres. I. Physicochemical characterization. *Journal of*
739 *biomedical materials research*, 42(1), 45-54.

740 Sarmiento, B., Ferreira, D., Veiga, F., & Ribeiro, A. (2006). Characterization of insulin-loaded alginate
741 nanoparticles produced by ionotropic pre-gelation through DSC and FTIR studies. *Carbohydrate Polymers*,
742 66(1), 1-7.

743 Shazly, G. A., Tawfeek, H. M., Ibrahim, M. A., Auda, S. H., & El-Mahdy, M. (2013). Formulation and evaluation
744 of fast dissolving tablets containing taste-masked microspheres of diclofenac sodium for sustained release.
745 *Digest Journal of Nanomaterials & Biostructures (DJNB)*, 8(3).

746 Song, C., Labhasetwar, V., Cui, X., Underwood, T., & Levy, R. J. (1998). Arterial uptake of biodegradable
747 nanoparticles for intravascular local drug delivery: results with an acute dog model. *Journal of controlled*
748 *release*, 54(2), 201-211.

749 Sunitha, S., & Amareshwar, P. (2010). Santhosh kumar M. a study on the effect of different cellulose
750 polymers on release rate from tramadol loaded microspheres prepared by emulsion solvent evaporation
751 method. *Asian Journal of Pharmaceutical and clinical research*, 3, 35-39.

752 Vichai V, Kirtikara K. (2006) Sulforhodamine B colorimetric assay for cytotoxicity screening. *Nature Protocols*
753 1, - 1112 - 1116

754 Wagh MA, Kothawade DP, Salunkhe KS, Chavan NV & Daga VR. (2011) Techniques used in orally
755 disintegrating drug delivery system. *International journal of drug delivery*,2(2).

756 Wei, Q., Yang, F., & Luan, L. (2013). Preparation and in vitro/in vivo evaluation of a ketoprofen orally
757 disintegrating/sustained release tablet. *Drug development and industrial pharmacy*, 39(6), 928-934.

758 Wu, Y., Yang, W., Wang, C., Hu, J., & Fu, S. (2005). Chitosan nanoparticles as a novel delivery system for
759 ammonium glycyrrhizinate. *International journal of pharmaceutics*, 295(1), 235-245.

760 Zhang, H. L., Wu, S. H., Tao, Y., Zang, L. Q., and Su, Z. Q. (2010). Preparation and characterization of water-
761 soluble chitosan nanoparticles as protein delivery system. *Journal of Nanomaterials*, 2010, 1